

Binding of a Designed Substrate Analogue to Diisopropyl Fluorophosphatase: Implications for the Phosphotriesterase Mechanism

Marc-Michael Blum,[†] Frank Löhr,[†] Andre Richardt,[‡] Heinz Rüterjans,^{*,†} and Julian C.-H. Chen^{*,†}

Contribution from the Institute of Biophysical Chemistry, J.W. Goethe University Frankfurt, Max-von-Laue-Strasse 9, D-60438 Frankfurt, Germany, and Armed Forces Scientific Institute for Protection Technologies—NBC Protection, D-29633 Munster, Germany

Received March 20, 2006; E-mail: chen@chemie.uni-frankfurt.de; hrueat@bpc.uni-frankfurt.de

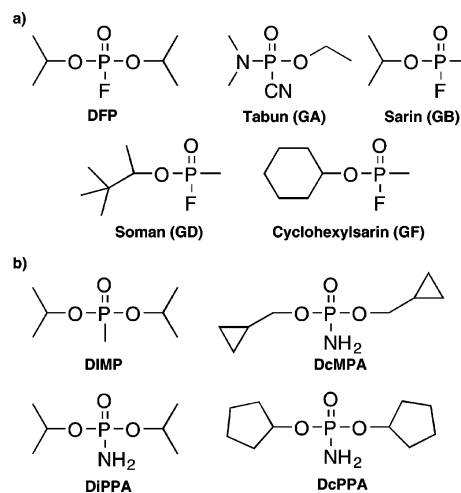
Abstract: A wide range of organophosphorus nerve agents, including Soman, Sarin, and Tabun is efficiently hydrolyzed by the phosphotriesterase enzyme diisopropyl fluorophosphatase (DFPase) from *Loligo vulgaris*. To date, the lack of available inhibitors of DFPase has limited studies on its mechanism. The de novo design, synthesis, and characterization of substrate analogues acting as competitive inhibitors of DFPase are reported. The 1.73 Å crystal structure of *O,O*-dicyclopentylphosphoroamidate (DcPPA) bound to DFPase shows a direct coordination of the phosphoryl oxygen by the catalytic calcium ion. The binding mode of this substrate analogue suggests a crucial role for electrostatics in the orientation of the ligand in the active site. This interpretation is further supported by the crystal structures of double mutants D229N/N120D and D229N/N175D, designed to reorient the electrostatic environment around the catalytic calcium. The structures show no differences in their calcium coordinating environment, although they are enzymatically inactive. Additional double mutants E21Q/N120D and E21Q/N175D are also inactive. On the basis of these crystal structures and kinetic and mutagenesis data as well as isotope labeling we propose a new mechanism for DFPase activity. Calcium coordinating residue D229, in concert with direct substrate activation by the metal ion, renders the phosphorus atom of the substrate susceptible for attack of water, through generation of a phosphoenzyme intermediate. Our proposed mechanism may be applicable to the structurally related enzyme paraoxonase (PON), a component of high-density lipoprotein (HDL).

Introduction

Diisopropyl fluorophosphatase from the squid *Loligo vulgaris* (DFPase, EC 3.1.8.2, 35 kDa) efficiently detoxifies highly toxic organophosphorus compounds that act as suicide inhibitors of acetylcholinesterase. Besides the compound diisopropylfluorophosphate (DFP), the enzyme also detoxifies the range of G-type nerve agents including Tabun (GA), Sarin (GB), Soman (GD), and Cyclohexylsarin (GF)^{1–3} (Chart 1a). Detoxification is achieved by hydrolysis of the bond between phosphorus and the fluoride or cyanide leaving group. DFPase is remarkably stable and can be highly expressed, making it a top candidate for enzymatic decontamination of chemical warfare agents.⁴

According to the enzyme classification of the International Union of Biochemistry and Molecular Biology (IUBMB), organophosphorus-hydrolyzing enzymes are found within class EC 3.1.8 (phosphotriesterases), although these enzymes show wide biochemical and sequence diversity. As nerve agents are

Chart 1



(a) Substrates of DFPase. Nerve agents are indicated by their common names and U.S. two-letter abbreviations; (b) compounds screened for interaction with DFPase.

synthetic compounds, they are not the native substrates of these enzymes. Several enzymes with activities against toxic organophosphorus compounds have been reported but only DFPase from *L. vulgaris*, organophosphorus hydrolase (OPH) from

[†] Institute of Biophysical Chemistry.

[‡] Armed Forces Scientific Institute for Protection Technologies—NBC Protection.

(1) Hartleib, J.; Rüterjans, H. *Protein Expression Purif.* **2001**, *21*, 210–219.
 (2) Scharff, E. I.; Koepke, J.; Fritsch, G.; Lucke, C.; Rüterjans, H. *Structure (Cambridge, MA, U.S.)* **2001**, *9*, 493–502.
 (3) Hoskin, F. C. G.; Roush, A. H. *Science* **1982**, *215*, 1255–1257.
 (4) Yang, Y. C.; Baker, J. A.; Ward, J. R. *Chem. Rev.* **1992**, *92*, 1729–1743.

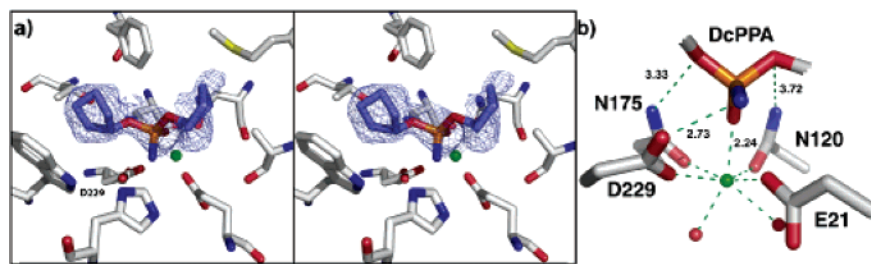


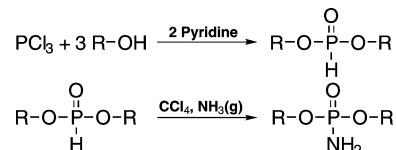
Figure 1. (a) Stereoview of DcPPA in the DFPase active site with F_0-F_c simulated annealing omit map, contoured at 2.5σ , calculated in CNS by omitting the inhibitor from the structure factor calculation. (b) Interaction of the substrate analogue DcPPA with DFPase. Potential hydrogen bond distances are indicated in Å, as well as the catalytic calcium-phosphoryl oxygen distance. The figure was generated using PYMOL (<http://pymol.sourceforge.net>).

Pseudomonas diminuta,^{5,6} and organophosphorus acid anhydrase (OPAA) from *Alteromonas*^{7,8} can be expressed in kilogram quantities, are stable, and show the catalytic rate enhancements required for rapid decontamination. Interestingly, the mammalian enzyme paraoxonase (PON, EC 3.1.8.1), a high-density lipoprotein (HDL) component⁹ that may function to inactivate toxic byproducts of lipid oxidation by the low-density lipoprotein (LDL) complex, is structurally related to DFPase and shows activity against organophosphate triesters.¹⁰ Although the natural function of squid type DFPase and *Pseudomonas* OPH is unknown, the *Alteromonas* OPAA has the function of a prolidase (E.C. 3.4.13.9).¹¹

Squid-type DFPase from *L. vulgaris*, which is the subject of this work, was originally isolated from squid head ganglion. The enzyme consists of 314 amino acids and contains two calcium ions. DFPase has been overexpressed in *E. coli* and purified,¹ and bulk quantities are readily available from expression in the yeast *P. pastoris*. Crystal structures of the DFPase apoenzyme have been solved at 1.8 Å and 0.85 Å resolution.^{2,12} The overall structure resembles a six-bladed pseudosymmetrical β -propeller with a central water filled tunnel. A high affinity calcium ion is located in the center of the molecule and has a structural role, while the second, low-affinity calcium ion is essential for catalytic activity and is located at the base of the active site, sealing the water filled tunnel (Figure 1a).

The low affinity calcium ion is crucial for catalysis, as removal of this metal ion results in a folded, yet inactive enzyme.¹³ From the X-ray structure and mutagenesis experiments, H287 in the active site was postulated to be essential for catalysis, acting as a general base. On the basis of these findings, a reaction mechanism for DFPase was proposed. The substrate coordinates the calcium ion via the phosphoryl oxygen, such that the fluoride leaving group points away from H287. The histidine then activates water by proton abstraction, allowing for a backside attack of the nucleophile on the phosphorus. From the pentacoordinate transition state, a fluoride ion leaves as the first product followed by the phosphoric acid anion. However,

Scheme 1. Synthetic Route to *O,O*-Dialkylphosphoramidates Employing the Todd–Atherton Reaction



very recent investigations have shown that this proposed mechanism is probably incorrect, as a number of H287 mutants still displayed substantial activity.¹⁴ Examples include H287F and H287L that show specific activities of 154 U/mg and 124 U/mg compared to the wild type activity of 194 U/mg. Water activation by these newly introduced amino acid residues is clearly not possible.

Since the substrates for DFPase are rapidly hydrolyzed, attempts to characterize substrate binding to DFPase have not been possible to date. As substrate analogues acting as enzyme inhibitors and their structural characterization are indispensable tools for studying enzyme reaction mechanisms, we sought to design inhibitors of DFPase and investigate their interactions with the protein. We report the de novo design and synthesis of a DFPase substrate analogue that functions as a competitive inhibitor and the 1.73 Å crystal structure of the inhibitor *O,O*-dicyclopentylphosphoramidate bound to DFPase. We further characterize its binding mode in the active site through a combination of NMR, kinetic, and computational techniques. On the basis of these data, we propose an alternative reaction mechanism, involving calcium coordinating residue D229 as a nucleophile and a phosphoenzyme intermediate which existence is proven by ¹⁸O labeling experiments.

Materials and Methods

Docking. Docking studies were carried out employing the software AUTODOCK3¹⁵ with low energy conformers of the ligands obtained with the CORINA program.¹⁶

Ligand Synthesis. The synthetic route to dialkylphosphoramidates is straightforward using the dialkylphosphite¹⁷ as an intermediate with a subsequent Todd–Atherton reaction¹⁸ to the dialkylphosphoramidate (Scheme 1). (Supporting Information)

Expression and Purification of DFPase. DFPase was expressed and purified according to previously published procedures¹ and is described in detail in the Supporting Information.

- (5) Munnecke, D. M. *Appl. Environ. Microb.* **1976**, *32*, 7–13.
- (6) Dumas, D. P.; Caldwell, S. R.; Wild, J. R.; Raushel, F. M. *J. Biol. Chem.* **1989**, *264*, 19659–19665.
- (7) Defrank, J. J.; Cheng, T. C. *J. Bacteriol.* **1991**, *173*, 1938–1943.
- (8) Cheng, T. C.; DeFrank, J. J.; Rastogi, V. K. *Chem.-Biol. Interact.* **1999**, *119–120*, 455–462.
- (9) Gaidukov, L.; Tawfik, D. S. *Biochemistry* **2005**, *44*, 11843–11854.
- (10) Harel, M.; Aharoni, A.; Gaidukov, L.; Brumshtein, B.; Khersonsky, O.; Meged, R.; Dvir, H.; Ravelli, R. B.; McCarthy, A.; Tokor, L.; Silman, I.; Sussman, J. L.; Tawfik, D. S. *Nat. Struct. Mol. Biol.* **2004**, *11*, 412–419.
- (11) Cheng, T. C.; Harvey, S. P.; Chen, G. L. *Appl. Environ. Microb.* **1996**, *62*, 1636–1641.
- (12) Koepke, J.; Scharff, E. I.; Lucke, C.; Ruterjans, H.; Fritsch, G. *Acta Crystallogr., Sect. D: Biol. Crystallogr.* **2003**, *59*, 1744–1754.
- (13) Hartleb, J.; Geschwindner, S.; Scharff, E. I.; Ruterjans, H. *Biochem. J.* **2001**, *353*, 579–589.

- (14) Katsemi, V.; Lucke, C.; Koepke, J.; Lohr, F.; Maurer, S.; Fritsch, G.; Ruterjans, H. *Biochemistry* **2005**, *44*, 9022–9033.
- (15) Morris, G. M.; Goodsell, D. S.; Halliday, R. S.; Huey, R.; Hart, W. E.; Belew, R. K.; Olson, A. J. *J. Comput. Chem.* **1998**, *19*, 1639–1662.
- (16) Sadowski, J.; Gasteiger, J. *Chem. Rev.* **1993**, *93*, 2567–2581.
- (17) Teichmann, B. *J. Prakt. Chem.* **1965**, *4. Reihe*, 94–98.
- (18) Atherton, F. R.; Openshaw, H. T.; Todd, A. R. *J. Chem. Soc.* **1945**, 660–663.

Table 1. Enzyme Kinetics and Inhibition

	WT	WT + DcPPA (1 mM)	WT + DcPPA (3 mM)	DcPPA
K_m (mM)	2.72 ± 0.05	23.36 ± 0.07	65.45 ± 0.13	
k_{cat} (s ⁻¹)	2107 ± 9	2111 ± 7	2091 ± 14	
k_{cat}/K_m (M ⁻¹ s ⁻¹)	0.77 × 10 ⁶	0.09 × 10 ⁶	3.19 × 10 ⁵	
K_i (μM)				125 ± 12
D229N/N120D	<1 U/mg			
D229N/N175D	<1 U/mg			
E21Q/N120D	<1 U/mg			
E21Q/N175D	<1 U/mg			

NMR Ligand Screening. For saturation transfer difference (STD) and WATER-LOGSY measurements, samples typically contained 100 μM DFPase, 1–2 mM inhibitor, in 10 mM Tris pH 7.5, 2 mM CaCl₂, 20% D₂O. Spectra were recorded at 277 K on a Bruker Avance 700 MHz equipped with a cryogenic ¹H{¹³C,¹⁵N} triple resonance probe. For the STD, saturation of the protein was achieved by a sequence of 50 ms WURST-20 pulses (1000 Hz sweep) applied for a total duration of 2 s at an offset of 9.7 ppm. For the WATER-LOGSY, selective inversion of the water was achieved by a 12 ms Gaussian shaped 180 degree pulse, with a mixing time of 1.5 s. In both cases, protein signals were suppressed by a 60 ms spin lock pulse.

Proton decoupled ³¹P NMR experiments were performed on a Bruker Avance 600 spectrometer, operating at 242 MHz ³¹P Larmor frequency. Measurements were done at 278 and 300 K using a conventional ¹H{¹³C, ³¹P} triple resonance probe. The protein/ligand ratio was varied from 0 (no protein) to 2; the maximum ligand concentration used was 3 mM; maximum protein concentration was 2.1 mM, in the same buffer as above.

For the detection of intermolecular NOEs, a 0.5 mM [^U-²H,¹⁵N] labeled DFPase, in 10 mM Bis-Tris-propane pH 6.5, 2 mM CaCl₂, containing 1 mM DCPA was employed. A 3D NOESY-¹⁵N,¹H]-TROSY spectrum was recorded at 275 K on a 900 MHz Bruker Avance spectrometer equipped with a cryogenic ¹H{¹³C,¹⁵N} triple resonance probe, using a mixing time of 300 ms.

Kinetic Measurements. The kinetic parameters K_m and k_{cat} of DFP hydrolysis were determined by pH stat assays. All measurements were carried out at 298 K in a nitrogen atmosphere. The total volume was 3.0 mL, at pH 7.5, containing 10 mM NaCl and 10% acetonitrile, and the reaction was initiated by addition of 2 μL of 0.5 mg/mL DFPase (28.57 pmol). Initial velocities v_0 were determined at eight different substrate concentrations (0.5–10 mM) in the absence and presence of 1 mM and 3 mM dicyclopentylphosphoramidate and corrected by the uncatalyzed rate of DFP hydrolysis. The kinetic parameters K_m and k_{cat} were determined by nonlinear least-squares fitting of the data to the Michaelis–Menten equation using the program MATHEMATICA 5. The inhibitory constant K_i was obtained from fitting of the data to the general inhibition equation. The parameters described are the average of at least three independent measurements (Table 1).

Single and Multiple Turnover Reactions of DFPase in H₂¹⁸O. For a typical multiple turnover experiment 10 nmol of DFPase in 50 μL MOPS buffer (50 mM, pH 8.0) were lyophilized. The reaction was started by dissolving the dried enzyme in 50 μL of H₂¹⁸O containing 1 μmol of DFP and incubated at room temperature for 6 h. For a single turnover experiment, 200 nmol of DFPase in 50 μL MOPS buffer (50 mM, pH 8.0) were lyophilized. The reaction was initiated by dissolving the dried enzyme in 50 μL of H₂¹⁸O containing 20 nmol of DFP and incubated at room temperature for 6 h.

After incubation, the reaction mixtures were ultrafiltered to remove the enzyme, diluted 10-fold with 50% acetonitrile/H₂O (1:1) and introduced into the mass spectrometer using a Harvard Apparatus syringe infusion pump operating at a flow rate of 5 μL/min. The molecular mass of the produced diisopropylphosphate was measured with an Applied Biosystems 4000 Q TRAP LC/MS/MS mass spectrometer equipped with an ionspray ion source in the negative ion mode (ion spray voltage = -4 kV; decluster potential = -15 V; entrance potential = -10 V).

Enzyme Digestion and LC/MS Analysis. A total of 10 nmol of DFPase in 50 μL MOPS buffer (50 mM, pH 8.0) was lyophilized. The reaction was started by dissolving the dried enzyme in 50 μL of H₂¹⁸O and adding 1 μmol of DFP (one control sample was prepared without the addition of DFP). The samples were incubated at room temperature for 12 h. Afterward, the samples were lyophilized again and dissolved in ammonium carbonate buffer (25 mM, pH 7.8). Endoproteinase Glu-C (Roche) was added (weight ratio 1:50), and the samples were incubated at 25 °C for 12 h.

The proteolytic digest was diluted 10-fold with ammonium formate buffer (final concentration 5 mM), loaded onto a Merck LiChroCART Supersphere 60 column connected to an Applied Biosystems 4000 Q TRAP mass spectrometer and then eluted with a linear gradient of 10–90% of 80% acetonitrile in 5 mM ammonium formate over 60 min at a flow rate of 200 μL/min. The ionspray ion source was operated in negative ion mode.

Crystallization, Structure Determination, and Refinement. Crystals of the free enzyme, D229N/N120D, and D229N/N175D mutants were grown at room temperature from ~38 mg/mL (~1 mM) protein in G150 buffer (10 mM Tris pH 7.5, 150 mM NaCl, 2 mM CaCl₂) by the hanging drop method. For crystals of the complex, 2 mM DFPase was mixed with a 60 mM stock solution of inhibitor dissolved in G150 buffer to a final concentration of 12 mM inhibitor. Crystals were obtained by mixing 2 μL of the protein solution with 2–3 μL of well solution, containing 10–15% PEG 6000, 0.1 M MES pH 6.5, and large crystals appeared after 2–3 days.

Data were collected at room temperature from capillary mounted crystals, on a rotating anode source, using Cu Kα radiation (1.5418 Å) and were recorded on a Mar Research 345 image plate. For the D229N/N175D mutant, data were collected at 100 K on DESY beamline BW-6 (1.05 Å) and recorded on a Mar CCD detector. Data were integrated, reduced, and scaled with Denzo/Scalepack (free enzyme and complex),¹⁹ and MOSFLM/SCALA (D229N/N175D).²⁰ For all datasets, integrated intensities were converted into structure factors using TRUNCATE (CCP4)²⁰ and converted into CNS format.²¹

Molecular replacement was done using the 100 K WT structure (PDB code 1E1A),² excluding the waters and the two calcium ions. Search models for the mutant structures used alanines in the positions of the mutated residues. Rotation and translation searches were performed in CNS or MOLREP. Manual building in CHAIN²² and Coot²³ was followed by rounds of positional, individual B-factor, and simulated annealing refinement in CNS to yield the final refined structures (Table 2).

For the cocrystal in the presence of 12 mM inhibitor, a difference Fourier F_o-F_c map was calculated based on phases from the room-temperature WT structure, yielding a greater than 12 σ peak for the position of the phosphorus atom of the inhibitor. A 7 σ contoured map showed a tetrahedral shaped peak, allowing for unambiguous placement of the oxygen and nitrogen atoms bonded to the phosphorus.

Coordinates of the solved structures have been deposited in the PDB under accession numbers 2GVU, 2GVV, 2GVW, and 2GVX.

Results

Inhibitor Design, Synthesis, and Characterization. To design an effective inhibitor, replacement of the labile fluoride leaving group by a moiety resistant to hydrolysis was necessary. Dialkylphosphoramidates were chosen, as earlier work with

(19) Otwinowski, Z.; Minor, W. *Macromol. Crystallogr., Part A* **1997**, *276*, 307–326.

(20) Bailey, S. *Acta Crystallogr., Sect. D: Biol. Crystallogr.* **1994**, *50*, 760–763.

(21) Brunger, A. T.; Adams, P. D.; Clore, G. M.; DeLano, W. L.; Gros, P.; Grosse-Kunstleve, R. W.; Jiang, J. S.; Kuszewski, J.; Nilges, M.; Pannu, N. S.; Read, R. J.; Rice, L. M.; Simonson, T.; Warren, G. L. *Acta Crystallogr., Sect. D: Biol. Crystallogr.* **1998**, *54* (5), 905–921.

(22) Sack, J. S. *J. Mol. Graphics* **1988**, *6*, 224–225.

(23) Emsley, P.; Cowtan, K. *Acta Crystallogr., Sect. D: Biol. Crystallogr.* **2004**, *60*, 2126–2132.

Table 2. Data Collection and Refinement Statistics

	WT	WT + inhibitor	D229N/N120D	D229N/N175D
source	rotating anode			DESY BW-6
wavelength	1.5418 Å			1.05 Å
temp	RT	RT	RT	100 K
resolution (Å)	1.86	1.73	1.9	2.39
R_{sym}	0.056	0.061	0.119	0.134
completeness	92.1%	94.2%	85.0%	100%
space group	$P2_12_12_1$			
unit cell (Å) <i>a</i>	43.4	43.6	43.4	42.6
<i>b</i>	83.3	83.0	83.2	82.7
<i>c</i>	87.5	87.5	87.3	86.7
reflections	25610	31969	21672	16354
R_{free}	20.8	21.6	24.3	27.1
R_{cryst}	17.8	18.7	18.1	22.0

the commonly used nerve agent mimic diisopropyl-methylphosphonate (DIMP) was unsuccessful, although it had been successfully cocrystallized with OPH.²⁴ Computational docking experiments using AUTODOCK3¹⁵ suggested that diisopropylphosphoramidate (DiPPA) should have a stronger binding affinity than DFP and DIMP. As the isopropyl groups of all these compounds do not fully occupy the hydrophobic side pockets of the active site, other groups were computationally screened employing bulkier side chains. The optimum binding affinity was predicted with cyclopentyl and cyclohexyl side chains, and steric factors led to poorer binding with bulkier side groups. Three different substrate mimics were therefore synthesized (Scheme 1) as potential inhibitors: DiPPA, dicyclopropylmethyl-phosphoramidate (DcPMPA), and dicyclopentylphosphoramidate (DcPPA) (Chart 1b).

Ligand binding was assessed by STD²⁵ and WATER-LOGSY²⁶ NMR experiments. DIMP showed no observable binding, while all three synthesized compounds show a clear STD effect. By using mixtures of two of the three compounds the relative binding affinities were deduced as the stronger binder always displaces the weaker one from the binding site. The WATER-LOGSY further characterizes the two binding compounds; the weaker binder gives rise to a negative signal, characteristic of displacement by the stronger binder, which has a positive signal. On the basis of these two methods, the three compounds were ranked in terms of their relative affinities, from weakest to strongest: DiPPA, DcPMPA, DcPPA.

The strongest inhibitor, DcPPA, was further characterized by measurement of the K_d by NMR, and kinetic measurements to measure its K_i and the effect of the inhibitor on the k_{cat} and K_m of DFPase (Table 1). The K_d was estimated to be 400 μM (water as solvent), and the K_i was measured to be 131 μM (water plus 10% acetonitrile as solvent). The measured k_{cat}/K_m of the free enzyme is 3-fold higher than those measured previously,²⁷ and is most likely due to a different solvent (ethanol vs acetonitrile).

Crystal Structure. The crystal structure of DFPase cocrystallized with the substrate analogue DcPPA was solved at 1.73 Å resolution, and refined to an R_{free} of 21.6%. The room-temperature structure of the DFPase free enzyme was solved to 1.86 Å resolution, and refined to a R_{free} of 20.9% (Table 2). The structures of the complex and of the room-temperature free

enzyme are nearly identical, although a minor rearrangement of the side chains of M148 and R146 in the active site leads to a slight expansion of the pocket. As such, there is remarkably little change in the enzyme conformation upon ligand binding, a textbook example of the lock and key model.

The ligand adopts an orientation in which its phosphoryl oxygen replaces a water molecule in the first coordination shell of the catalytic calcium; the amino group of the ligand is oriented toward H287, while the phosphoryl oxygen coordinates the calcium ion (Figure 1b). The aliphatic rings of the ligand are involved in van der Waals contacts with the side chains of the active site residues. There is one weak hydrogen bond (3.33 Å $\delta\text{O}-\text{N}$) between the δ oxygen of the ligand and one of the side chain amide protons of N175. Although the position of the phosphoramidate hydrogens are equivocal, there are possible hydrogen bond interactions with the carboxylate oxygens of E21 (2.78 Å) and D229 (2.73 Å). None of the interactions between protein and ligand are bridged by water molecules, and the ligand fully occupies the active site. The phosphoryl oxygen–calcium distance in the complex is remarkably short, 2.24 Å (Figure 1c). Interestingly, this is the same as the phosphate oxygen–calcium distance reported in PON,¹⁰ involving the negatively charged phosphate (cf. the uncharged DcPPA). Thus, the short distance observed in our structure is strongly suggestive of substrate activation, by electron withdrawal from the phosphorus atom.

A priori, because of the symmetry of the ligand, there are two possible interactions between the calcium and the available coordinating atoms of the ligand, with either a calcium–amide nitrogen interaction, or a calcium–oxygen interaction. In X-ray structures it is difficult to distinguish nitrogen from oxygen (7 vs 8 electrons). It has been modeled as a calcium–oxygen interaction for several reasons. First, the coordination environment of calcium is strongly biased toward calcium–oxygen interactions, according to the theory of hard and soft acids and bases (HSAB).²⁸ Second, the phosphorus–oxygen bond length is expected to be shorter than the phosphorus–nitrogen bond length. In the crystal structure, the P–O distance is 1.48 Å, and the P–N distance is 1.62 Å. This is in good agreement with quantum mechanical studies of the free ligand in vacuo at the MP2/6-31G* level of theory using SPARTAN,^{29,30} where the P–O distance is 1.52 Å and the P–N distance is 1.64 Å. Third, intermolecular NOEs are observed between the NH_2 group of the inhibitor and the H287 side chain, indicative of their proximity. For these reasons, we have modeled the ligand with a calcium–phosphoryl oxygen coordination.

We only observe the orientation of the ligand where the nitrogen points toward H287 (Figure 1b). A second possible orientation with the nitrogen pointing toward F173 is not observed. In the previously proposed reaction mechanism the fluoride leaving group would be oriented toward F173 in order to allow the activated water to attack from H287.² In the crystal, the ligand displaces the C-terminal residue F314, contributed from a symmetry-related molecule. In spite of this, the specific binding mode of the ligand in the active site pocket, and the bond distances between the calcium and the phosphoryl oxygen, suggest that the interaction is neither an artifact of the crystallization nor a consequence of crystal packing.

(24) Benning, M. M.; Hong, S. B.; Raushel, F. M.; Holden, H. M. *J. Biol. Chem.* **2000**, *275*, 30556–30560.

(25) Mayer, M.; Meyer, B. *Angew. Chem., Int. Ed.* **1999**, *38*, 1784–1788.

(26) Dalvit, C.; Pevarello, P.; Tato, M.; Veronesi, M.; Vulpetti, A.; Sundstrom, M. *J. Biomol. NMR* **2000**, *18*, 65–68.

(27) Hartleib, J.; Ruterjans, H. *Biochim. Biophys. Acta* **2001**, *1546*, 312–324.

(28) Pearson, R. G. *J. Am. Chem. Soc.* **1963**, *85*, 3533–3539.

(29) *Spartan '04*; Wavefunction Inc.: Irvine, CA, 2004.

(30) Pople, J. A. et al. *J. Comput. Chem.* **2000**, *21*, 1532–1548.

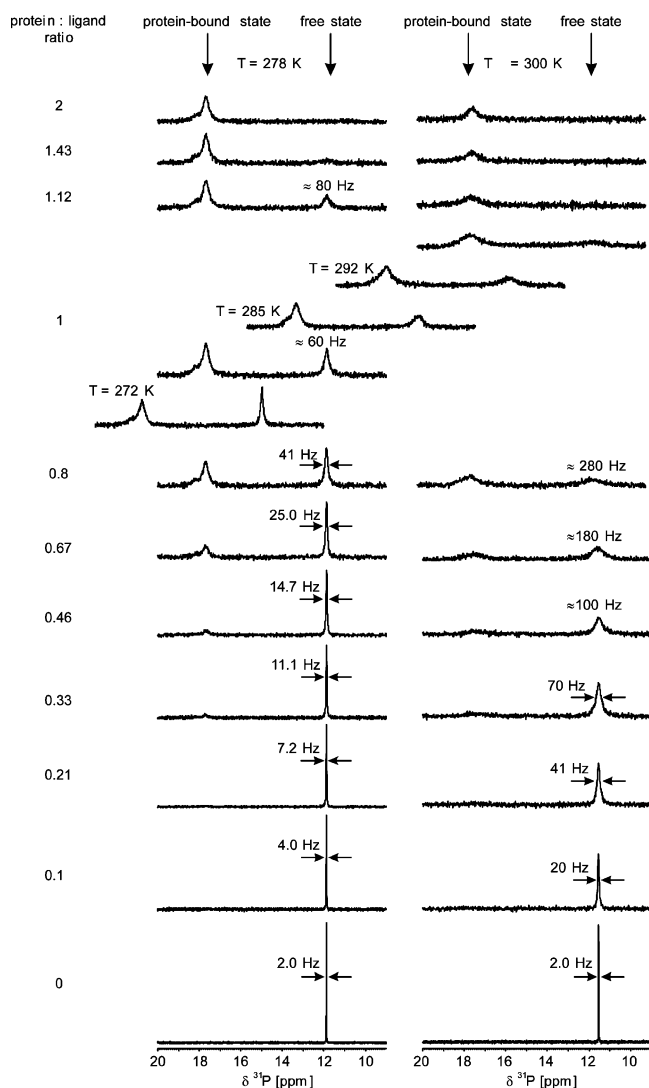


Figure 2. ^{31}P NMR titration of DcPPA with DFPase at 278 and 300 K. The protein/ligand ratio ranges from 0 to 2 as indicated on the left. For a 1:1 mixture, spectra were recorded at five different temperatures. Experiments were carried out at 242 MHz with the number of scans ranging from 2048 to 60000. Spectra are vertically scaled to obtain approximately equal noise levels. Line width (full width at half-height) of the free state signal are indicated where measurements were possible.

On a dynamic level, using ^{31}P NMR as a chemical probe, the inhibitor was titrated with unlabeled protein and measured at 278 and 300 K (Figure 2).

Upon addition of the protein, a second signal becomes detectable 5.8 ppm downfield from the free inhibitor. This downfield shift upon addition of protein can be explained by the polarization of the phosphorus–oxygen bond due to coordination to the calcium. This indicates that the calcium ion participates in substrate activation. Furthermore, the appearance of two separated signals is indicative of a slow exchange of the free and bound states on the NMR time scale, with an estimated upper limit of 1400 s^{-1} . In contrast, for fast chemical exchange, one would expect one signal at an averaged chemical shift which changes with the protein to ligand ratio. From the line broadening of the free state signal upon addition of DFPase, the exchange rate can be estimated as $250\text{--}300\text{ s}^{-1}$ at 278 K. Exchange broadening becomes more severe with increasing temperature (Figure 2).

^{18}O Incorporation Experiments. To prove the existence of a phosphoenzyme intermediate in the catalytic cycle of DFPase we have used ^{18}O labeling techniques. Following a similar approach to investigate the mechanism of L-2-haloacid dehalogenase,³¹ we investigated single and multiple turnover events of DFPase hydrolyzing DFP in H_2^{18}O . The single turnover enzyme reactions were carried out with an excess of enzyme, whereas the multiple turnover reactions were done using an excess amount of substrate. If the single turnover experiment reveals the incorporation of ^{16}O in the product, the reaction must proceed via a phosphoenzyme intermediate as the only source of ^{16}O in the solution is the enzyme itself. As the transferred ^{16}O is replaced by ^{18}O after the first turnover, further turnovers will result in the incorporation of ^{18}O . In case the reaction proceeds via the attack of activated water (either by an activating amino acid or the metal), ^{18}O will be incorporated in both the single and multiple turnover experiment. The results clearly show the incorporation of ^{16}O in the single turnover experiment compared with ^{18}O incorporation in the multiple turnover experiments (Figure 3). Therefore an oxygen atom must be transferred from the enzyme to the product during the course of the catalytic cycle, indicative of a phosphoenzyme intermediate.

To identify the amino acid residue that is acting as a nucleophile the protein was digested using endoproteinase Glu-C. For this experiment DFPase was lyophilized and H_2^{18}O was added. DFP was added to start the reaction (multiple turnover) while there was no addition of DFP for the control reaction. After the reaction was completed, the protein was lyophilized again to remove H_2^{18}O and endoproteinase Glu-C was used for digestion. The fragment containing the residue D229 was the peptide with the sequence GGADGMDFDE, residues 221–230. Visual inspection of the position of the peptide fragment within the DFPase structure reveals that only D229 is located in the active site and is accessible by solvent. LC/MS analysis was used to identify the proteolytic fragments. Ion spray mass spectra shows the fragment of interest in negative ion mode at $m/z = 1013.6$ in the control sample. In the sample reacted with DFP, a signal with $m/z = 1018.1$ is visible at the same elution time while the original signal of $m/z = 1013.6$ is still detectable but with significantly reduced intensity. The signal with $m/z = 1018.1$ is not detectable in the control sample. The mass difference of 4 indicates that both carboxyl oxygens of D229 incorporated the isotope. This can be explained by the fact that the calcium ion has an off rate of $\sim 1\text{ s}^{-1}$.¹³ During the time the active site is without a bound metal, the carboxyl group of D229 is able to flip around.

Discussion

The orientation of the ligand suggests that the central “core” of the active site cleft is critical for guiding the ligand into the proper orientation. This core contains the catalytic calcium ion, coordinated by acidic residues E21 and D229 on one face, and N120 and N175 on the other, such that the ligand may be electrostatically oriented in the active site (Figure 1b). To test this possibility, four sets of double mutants were constructed, trying all chemically reasonable permutations, while preserving the charge balance of the calcium coordination environment. The double mutant D229N/N120D was found to be inactive,¹⁴ albeit with weak binding of DcPPA based on STD data. The

(31) Liu, J. Q.; Kurihara, T.; Miyagi, M.; Esaki, N.; Soda, K. *J. Biol. Chem.* **1995**, *270*, 18309–18312.

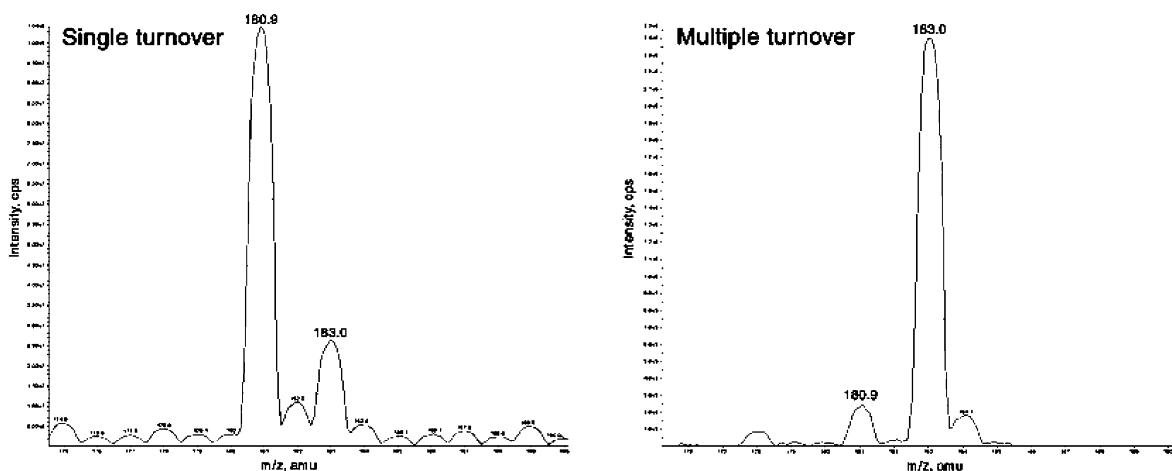


Figure 3. Ion spray mass spectra of diisopropylphosphate produced with DFPase in H_2^{18}O . The spectra were obtained between 175 and 195 atomic mass units. A single turnover cycle of DFPase yields ^{16}O -diisopropylphosphate $M_r = 181$ amu (left) while multiple turnovers result in ^{18}O incorporation $M_r = 183$ amu (right).

crystal structure of D229N/N120D was solved and refined at 1.9 Å resolution (Table 2). In the crystal structure, the active site environment is unchanged, notably in the calcium coordination environment. A second double mutant was constructed, D229N/N175D. This mutant also shows no activity, and surprisingly, no inhibitor binding was detected by NMR STD measurements, indicative of a significant effect of these mutations on the K_m . The crystal structure was solved at 2.4 Å resolution (Table 2). Like D229N/N120D, the D229N/N175D structure shows an unchanged calcium coordination environment and an undisturbed substrate binding pocket. Double mutants E21Q/N120D and E21Q/N175D also showed no activity (Table 1). These results strongly suggest that the correct electrostatic topography of the active site is absolutely necessary for binding and catalysis. Furthermore, these results significantly narrow down the basis for substrate recognition, binding, and enzymatic activity. Nevertheless, the hydrophobic ‘wings’ of the active site pocket are also important for binding, as DiPPA was a weak inhibitor while DcPPA was a better inhibitor (Figure 1a).

A number of studies have suggested the role of H287 as a general base.^{2,27} For this to occur, the hydroxide generated by proton abstraction by H287 must attack the phosphorus from a position apical to the fluoride leaving group. The amino group of the inhibitor DcPPA points toward H287 and this result is in very good agreement with the docking studies carried out using AUTODOCK (Figure 4). The docked conformation of DFP also shows the fluoride leaving group pointing toward H287 (Figure 5). In this orientation the backside attack of hydroxide is not possible. Together with the active H287L and H287F mutants reported previously, and the lack of pH titration effects for this residue,¹⁴ this rules out H287 as a general base.

We rule out the direct attack of hydroxide from bulk solvent. At the lower pH limit of stability (pH 5; $[\text{OH}^-] = 10^{-9}$ M) the hydroxide concentration is 10-fold lower than the enzyme concentration used in the kinetic experiments and is too small to account for the activity measured.²⁷ Furthermore, we rule out the possibility of direct activation of water by the catalytic calcium ion. Exchanges of the catalytic calcium ($K_d \approx 1 \mu\text{M}$) with Mg^{2+} and Ba^{2+} show a slight increase of activity by approximately 5–20% relative to the wild-type. Much stronger effects would be expected for the case where the metal ion acts as a water activator. Furthermore, mutants of all non-calcium-

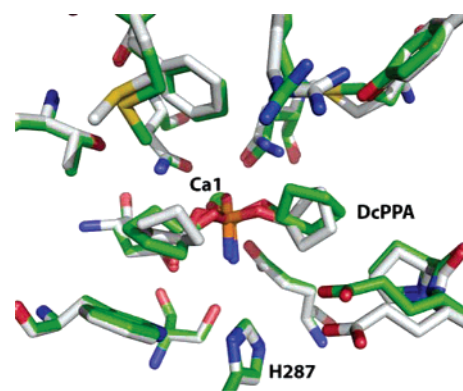


Figure 4. Aligned structures of DcPPA docked into the DFPase active site (green) and the structure of DcPPA in complex with DFPase as revealed by X-ray crystallography (gray). Only minor differences in the protein structure are visible upon binding.

coordinating amino acids with functional groups in the active site vicinity did not implicate any water activating residues.^{2,14}

We propose the following mechanism (Figure 6). The prerequisites are that the residue must be in an orientation such that an inline attack of a nucleophile upon the phosphorus can occur, and the only reasonable residue available for this is D229. D229 has one available oxygen exposed in the active site; the other oxygen is involved in coordinating the calcium.

As such, we propose that the D229 carboxylate plays a dual role, in coordinating the calcium ion, and acting as the nucleophile. This is similar to that proposed for the phosphatase activity in epoxide hydrolase^{32a} where the nucleophilic aspartate is coordinated to magnesium and to that proposed for phosphonoacetaldehyde hydrolase from *Bacillus cereus*.^{32b} In general, metal dependent phosphatase activities of enzymes belonging to the haloacid dehalogenase (HAD) superfamily are thought to work via an enzyme aspartate coordinated to the magnesium nucleophile.³³ Although the coordination of D229 to the calcium ion should lower the nucleophilicity of the carboxylate, this effect may be balanced by the coordination of the phosphoryl

(32) (a) Gomez, G. A.; Morisseau, C.; Hammock, B. D.; Christianson, D. W. *Biochemistry* **2004**, *43*, 4716–4723. (b) Morais, M. C.; Zhang, W. H.; Baker, A. S.; Zhang, G. F.; Dunaway-Mariano, D.; Allen, K. N. *Biochemistry* **2000**, *39*, 10385–10396.

(33) Allen, K. N.; Dunaway-Mariano, D. *Trends Biochem. Sci.* **2004**, *29*, 495–503.

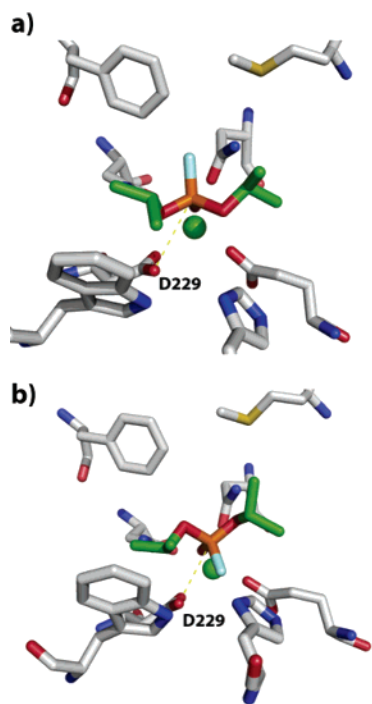


Figure 5. Docking studies reveal productive (a) and nonproductive (b) binding of DFP in the DFPase active site. The difference of the two states is estimated to be about 0.5 kcal/mol. Nucleophilic inline attack of D229 on the phosphorus is possible in structure (a) but not in structure (b) as the leaving group points in the wrong direction.

oxygen to the calcium. Car–Parrinello molecular dynamics on the crucial reaction step in the phosphatase activity of exo-2,3-epoxide hydrolase leading toward the formation of the phosphoenzyme intermediate showed clearly that such a step is possible.³⁴ The comparatively slow k_{cat} for DFPase may be reflective of an equilibrium between the nonproductive and productive orientations of the ligand in the binding pocket. We suggest that the DFP substrate is bound in two orientations, a nonproductive one similar to that seen in the inhibitor/enzyme cocrystal structure, with the fluorine atom pointing toward H287, in equilibrium with a productive orientation, where the fluorine is pointing away from D229 (Figure 5). On the basis of docking experiments, the productive orientation is estimated to be only 0.5 kcal/mol higher in energy than the nonproductive orientation.

The calcium ion is involved in activation of the substrate, rendering the phosphorus atom electron poor and therefore primed to attack by D229. Titration experiments with DcPPA show a shifted ^{31}P NMR spectrum, indicative of polarization of the phosphorus–oxygen bond by the calcium (Figure 2). D229 attacks the phosphorus atom, leading to the release of fluoride and generating a phosphoenzyme intermediate. This process is possibly assisted by hydrogen bonding of the fluorine to the amide group of N120. In the second step, the carboxylate carbon of D229 is attacked by a water molecule, leading to the hydrolysis of the D229–phosphoenzyme bond under transfer of an oxygen atom from D229 to the product diisopropylphosphate, regeneration of the D229, and product generation (Figure 6). The rate of hydrolysis of acetylphosphate is $\sim 10^{-4} \text{ s}^{-1}$ under physiological conditions. The turnover rate of DFPase is $\sim 200 \text{ s}^{-1}$. With no obvious general base in the vicinity, this is difficult to explain.

Proper arrangement of a water molecule for attack on the phosphoenzyme intermediate can contribute to a rate enhancement even without water activation.³⁵ Also it is important to note that the intermediate is not a charged acetyl phosphate but a neutral alkylated species. Involvement of the calcium ion in water activation at this step is highly unlikely because of steric reasons. Even if a water molecule could coordinate to calcium during the existence of the intermediate it would be too far away and poorly positioned for an attack on the carboxylic carbon of D229.

Electrostatics also plays a crucial role in substrate orientation, as all mutants switching the polarity of the calcium coordinating residues result in inactive enzyme. Two of these mutants are identical in structure to the wild-type enzyme, and show no change in the calcium coordination environment.

Docking studies of the binding of the substrate ethyl *N,N*-dimethyl phosphor-amidocyanidate (Tabun) give further support to the proposed mechanism. Because of the size and steric constraints of the linear cyano group, both enantiomers of Tabun³⁶ are able to bind in the DFPase active site, though neither with the cyano group pointing toward H287 (similar to the inhibitor DcPPA) nor directly away from it (similar to DFP in a previously proposed reaction mechanism²). Results of the docking show conformations where the cyano group is positioned for an inline attack of D229 on the phosphorus atom (Figure 7).

Our proposed mechanism makes several predictions, which can be tested experimentally. One key feature of the mechanism is the enzyme as the reactive nucleophile itself and not activated water leading to the formation of a phosphoenzyme intermediate. We were able to prove the existence of this intermediate by isotopic labeling using H_2^{18}O and analysis by mass spectroscopy (Figure 3). Also the pK_a of D229 is expected to be significantly altered because of the pH dependence of the reaction. Although an 0.85 Å X-ray structure of DFPase is available, it was not possible to assign the hydrogen atoms in the active site.¹²

As the medically important enzyme paraoxonase (PON) is structurally related to DFPase with both proteins showing propeller structures, two calcium ions, a water filled tunnel, and activity against phosphorus triesters, we investigated the crystal structure of an engineered PON1 available from the PDB (PDB code: 1V04) for possible mechanistic similarities.¹⁰ The currently proposed mechanism for PON1 suggests activation of water by a His–His dyad (H115, H134). Although recent work has shown that the His–His dyad is mediating the lactonase and esterase functions of PON1,³⁷ there are experimental results that suggest that the triesterase activity of PON1 might follow a different mechanism. Yeung et al. reported that the H115W mutant of PON1 retains activity with paraoxon.³⁸ They concluded that H115 is not directly involved in catalysis.³⁹ Close inspection of the coordination environment around the catalytic calcium reveals that the residue D269 could function as a nucleophile similar to D229 in DFPase. Substrates with large leaving groups like the nerve agent VX, for which a small activity was discovered,⁴⁰ are predicted to position their leaving

(34) De Vivo, M.; Ensing, B.; Klein, M. L. *J. Am. Chem. Soc.* **2005**, *127*, 11226–11227.

(35) Clausen, J. D.; McIntosh, D. B.; Woolley, D. G.; Andersen, J. P. *J. Biol. Chem.* **2001**, *276*, 35741–35750.

(36) Benschop, H. P.; Dejong, L. P. A. *Acc. Chem. Res.* **1988**, *21*, 368–374.

(37) Khersonsky, O.; Tawfik, D. S. *J. Biol. Chem.* **2006**, *281*, 7649–7656.

(38) Yeung, D. T.; Josse, D.; Nicholson, J. D.; Khanal, A.; McAndrew, C. W.; Bahnsen, B. J.; Lenz, D. E.; Cerasoli, D. M. *BBA-Proteins Proteom.* **2004**, *1702*, 67–77.

(39) Yeung, D. T.; Lenz, D. E.; Cerasoli, D. M. *FEBS J.* **2005**, *272*, 2225–2230.

(40) Broomfield, C. A.; Morris, B. C.; Anderson, R.; Josse, D.; Masson, P. *Conference Proceedings CBMTS III*, Spiez, Switzerland, May 2000.

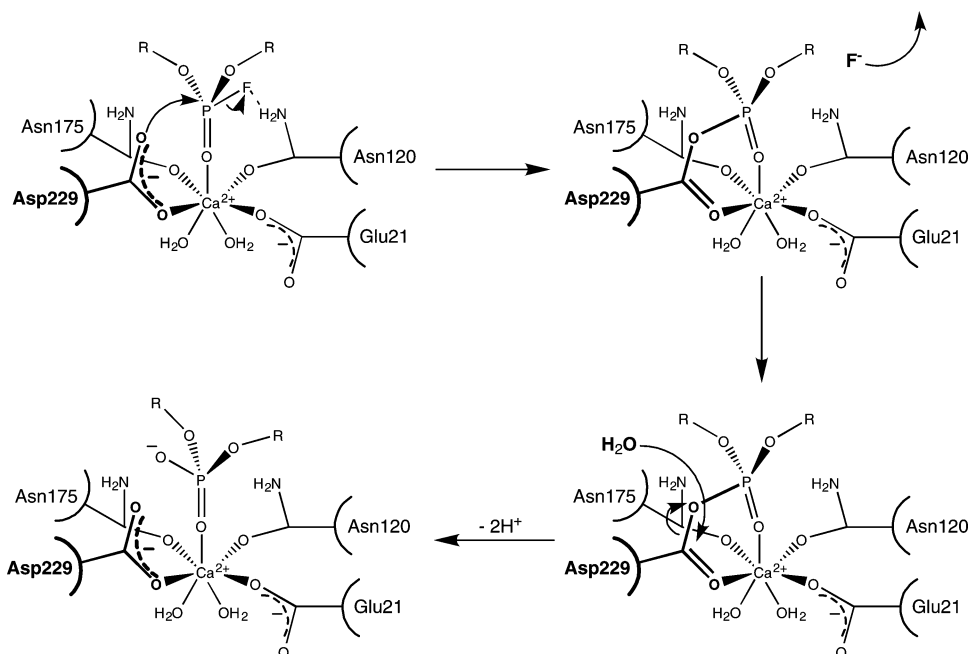


Figure 6. Proposed mechanism of DFP hydrolysis. After coordination of the substrate to the catalytic calcium ion, the phosphorus atom is subject to nucleophilic attack by D229, generating a phosphoenzyme intermediate, accompanied by release of fluoride, assisted by hydrogen bonding to N120. The intermediate is then attacked by water at the carboxylate carbon of D229 resulting in a transfer of oxygen from D229 to the phosphoric acid product leaving the active site as diisopropylphosphate.

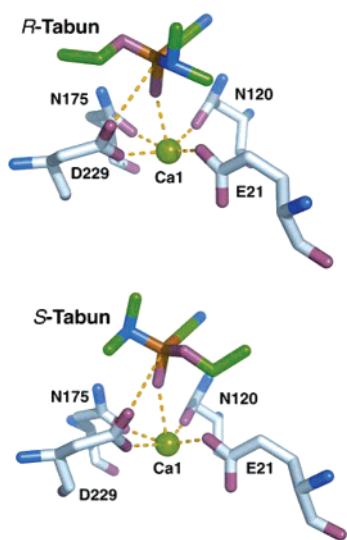


Figure 7. Results of computational docking of both enantiomers of Tabun in the DFPase active site. Docked conformations are those of lowest energy displaying a phosphoryl oxygen to calcium coordination. In both cases the cyanide leaving group of Tabun is oriented in a way that is well suited for an inline attack on the phosphorus by D229. Because of the size and steric constraints of the linear cyano group, Tabun is unable to bind to DFPase with the cyano group pointing toward H287 (like the inhibitor DcPPA) or pointing away from H287 (as proposed for DFP in the previously proposed reaction mechanism).

groups in an orientation such that water activated by the His–His dyad is unable to perform the necessary inline attack. In contrast, D269 is well positioned for this to occur (Figure 8).

Through the design and synthesis of a DFPase inhibitor, and its kinetic characterization, combined with computational, mutational, and structural studies, we have proposed a possible mechanism for the action of DFPase. A thorough understanding of the mechanism will be crucial for efforts aimed at large-scale enzymatic decontamination of existing nerve agent stocks, as well as re-

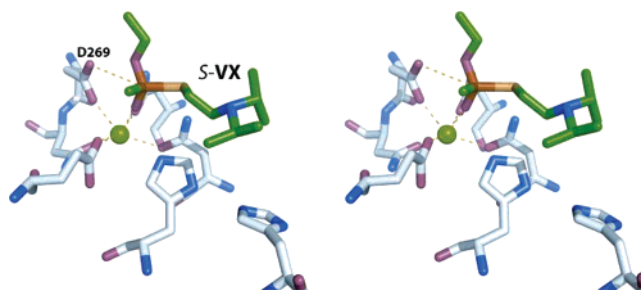


Figure 8. Docked conformation of VX in the active site of paraoxonase (PON). Residue D269 is well positioned for a nucleophilic attack on the phosphorus atom of VX.

engineering DFPase to expand the repertoire of compounds that can be detoxified by the enzyme, notably the nerve agent VX.⁴¹

Acknowledgment. We thank Gleb Bourenkov (DESY) and Roy Lancaster (MPI Biophysik) for access to X-ray facilities and assistance with data collection. We thank Hans-Jürgen Altmann, Werner Hörnemann (Armed Forces Research Institute for Protection Technologies), and Juliana Winkler (Frankfurt) for technical assistance, Harald John, Christian Becker, and Erwin Wagner (Armed Forces Institute of Pharmacology and Toxicology) for help with mass spectrometry, and Alex Koglin and Volker Dötsch for critical comments on the manuscript. This research was funded by Fraunhofer Grant E590/3X023/M5137 and by the Hessisches Ministerium für Wissenschaft und Kultur.

Supporting Information Available: General synthesis of substrate analogues, protein purification protocol, and complete ref 30. This material is available free of charge via the Internet at <http://pubs.acs.org>.

JA061887N

(41) Yang, Y. C. *Acc. Chem. Res.* **1999**, *32*, 109–115.